Limnol. Oceanogr., 55(5), 2010, 1821–1834

doi:10.4319/lo.2010.55.5.1821

Dead in the water: The fate of copepod carcasses in the York River estuary, Virginia

David T. Elliott,* Courtney K. Harris, and Kam W. Tang

Virginia Institute of Marine Science, College of William & Mary, Gloucester Point, Virginia

Abstract

Using laboratory and field experiments we investigated three fates of copepod carcass organic matter in the York River estuary, Virginia: ingestion by planktivores (necrophagy), microbial decomposition, and removal by gravitational settling in the presence of turbulence (sinking). The ctenophore *Mnemiopsis leidyi* ingested live copepods and carcasses indiscriminately in feeding experiments. Microbial decomposition led to ca. 50% of carcass dry weight loss within 8 h after death. Carcass settling velocities in still water were ca. 0.1 cm s^{-1}, implying short residence time (hours) in the shallow estuary. However, turbulent mixing kept carcasses in suspension much of the time, reducing sinking losses. Rates of carcass organic matter removal were combined in a simple mathematical model predicting the fate of estuarine copepod carcasses. When sinking was considered, it removed a large fraction of carcass organic matter ($\geq$ 58% for copepodites, $\geq$ 35% for nauplii), with most of the remainder being removed by microbial decomposition. In the absence of sinking losses, necrophagy became proportionally more important in removing carcass organic matter ($\geq$ 49%, except in summer).

Studies of marine zooplankton population abundance rarely consider the vital status of the animals collected. However, zooplankton carcasses can at times comprise 10% or more of the total individuals in field samples (reviewed by Elliott and Tang [2009]). These carcasses likely result from non-predatory mortality, defined here as mortality in which individuals are not immediately ingested and for which there are causes such as injuries, resource limitation, disease, parasitism, harmful algal blooms, environmental stresses, or old age (Kimmerer and McKinnon 1990; Hall et al. 1995; Gomez-Gutierrez et al. 2003). Non-predatory mortality appears to be common among freshwater crustacean zooplankton (McKee et al. 1997; Gries and Güde 1999; Dubovskaya et al. 2003), but its importance in marine systems is poorly known because of the difficulty in measuring it. Nevertheless, a global analysis indicates that non-predatory factors account for 1/4 to 1/3 of the total mortality in marine planktonic copepods (Hirst and Kiørboe 2002), and the resultant carcasses represent a concentrated pool of labile organic substrates for microorganisms (Tang et al. 2006*b*, 2009), a potential food source for other organisms (Zajączkowski and Legeżyńska 2001), and a vehicle for transporting essential biomolecules, toxins, and pollutants (Lee and Fisher 1994; Frangoulis et al. 2005; Bickel and Tang 2010). Several recent studies indicate that copepod carcasses can at times represent a large fraction ($\sim$ 1/4–1/2) of total vertical downward flux of particulate organic carbon to the deep sea (Sampei et al. 2009; Frangoulis et al. in press). Hence, quantification of non-predatory mortality and the fate of the resulting carcasses are critical for understanding zooplankton population dynamics, ocean trophodynamics, and biogeochemistry.

Available data indicate that copepod carcasses may be common in marine and estuarine environments. Using neutral red stain to identify carcasses, Tang et al. (2006*a*) observed that, on average, 29% of collected copepods were dead during the summer of 2005 in the lower Chesapeake Bay, Virginia. Between 2007 and 2008, an average of 13–28% of collected copepods were found to be dead in the York River sub-estuary of Chesapeake Bay, and the percentage was higher among younger developmental stages (D. T. Elliott unpubl.). Non-predatory mortality rate for estuarine and oceanic copepods has been estimated to be ca. 0.1 d^{-1} (Mauchline 1998; Tang et al. 2006*a*), indicating that, on average, 10% of copepod production could be diverted to carcass-based trophic pathways.

The goal of the present study was to determine the fate(s) of copepod carcasses and associated organic matter in the York River estuary. A combined experimental, observational, and modeling approach was used to quantify rates of removal of carcass organic matter from the water column through ingestion by planktivores (necrophagy), microbial decomposition, and gravitational settling in the presence of turbulence (sinking losses).

Methods

Our study included three components: (1) Carcass removal: Laboratory experiments were conducted to determine the potential rates of removal of copepod carcasses via necrophagy, microbial decomposition, and gravitational settling. (2) Effects of turbulence: The likelihood that resuspension and turbulent diffusion prolong residence time of copepod carcasses in the water column was investigated by additional laboratory experiment and field sampling. (3) Fate of carcass organic matter: Results of these experiments and observations were combined with literature information and applied to a mathematical model that predicted the fate of copepod carcass organic matter under various environmental conditions in the York River estuary.

Study area—The York River is a partially mixed microtidal estuary, with depths ranging from 6 m to 20 m along the main channel, maximum tidal currents nearing

* Corresponding author: delliott@vims.edu

1 m s^{-1}, a tidal range of 0.7–0.85 m, and a typical bed stress of around 1.10 cm s^{-1} (Kim et al. 2000; Friedrichs 2009). Water temperatures in the York River range from 2°C to 31°C on an annual cycle (Reay and Moore 2009). Phytoplankton abundance and chlorophyll *a* concentration peak in the spring and summer, and primary production is high (60–70 mg C m^{-3} h^{-1}) from March through August (Marshall 2009). The dominant mesozooplankton taxa are copepods (Steinberg and Condon 2009). The calanoid copepod *Acartia tonsa* is dominant in the summer and is replaced by *Acartia hudsonica* in the winter, while *Eurytemora affinis* is more abundant in the spring and in the mesohaline portion of the estuary (Steinberg and Condon 2009). The ctenophore *Mnemiopsis leidyi* is present persistently throughout much of the York River, becoming particularly abundant at times (Steinberg and Condon 2009). *M. leidyi* and other gelatinous planktivores are the major predators of mesozooplankton in Chesapeake Bay, particularly during the summer (Baird and Ulanowicz 1989; Steinberg and Condon 2009).

Source of carcasses—Copepod carcasses for laboratory experiments were produced from live and active *A. tonsa* collected from the York River estuary. Animals were held in 20 salinity Instant Ocean artificial seawater (ASW) in polycarbonate bottles. Water temperature was slowly raised to 50°C and maintained for 5 min, after which the animals were collected onto a sieve and returned to ASW at room temperature. This procedure killed almost all copepods while keeping the carcasses intact. Intact carcasses were sorted by age class into nauplii, copepodite stages I to III (CI–CIII), and copepodite stages IV through adult (CIV–CVI).

Carcass removal: Ctenophore selectivity—The rate at which planktivores consume copepod carcasses was quantified using the ctenophore *M. leidyi* from the York River estuary as a model organism and testing for ctenophore selectivity between live copepods and carcasses. Incubations were performed using cydippid larvae (< 10-mm diameter) and adult *M. leidyi* (ca. 40-mm diameter). For acclimation, 20–30 similarly sized ctenophores were incubated in the dark for 24 h in ASW containing similar numbers of live copepods and carcasses at 20°C. Experiments with cydippid larvae consisted of triplicate 4-liter polycarbonate bottles of ASW at 20°C, each of which contained three cydippid larvae and either live or dead *A. tonsa* (CIV–CVI; 100 copepods per bottle). Triplicates of predator-free control were also set up to account for copepod and carcass loss during processing. Adult ctenophore incubations were modified to include one ctenophore with both live copepods and carcasses in equal amounts (50 + 50 total per bottle) in each 4-liter bottle. To distinguish between live copepods and carcasses in these mixed treatments, live copepods were stained with neutral red and mixed with unstained carcasses in three replicate bottles, and stained carcasses were mixed with unstained live copepods in another three replicate bottles. The separate staining of live copepods and carcasses was accomplished in order to control for possible preferential ingestion or rejection of individuals as a result of the stain. Live copepods were stained with a 1 : 670,000 stain concentration (10% of concentration recommended by Elliott and Tang [2009]) for 3 min; afterward, the copepods remained alive, active, and visibly stained for the duration of the incubations (2–4 h). Stained carcasses were prepared by immersing live copepods in a 1 : 33,500 stain concentration (200% concentration recommended by Elliott and Tang [2009]) for 15 min, after which animals were heat killed while still in the staining solution. The resulting carcasses were visibly stained for ~ 6 h.

To begin feeding experiments, acclimated ctenophores were introduced into bottles with known amounts of copepods and carcasses and incubated in the dark on a plankton wheel (2 revolutions per min, rpm) for 2–4 h. At the end of the incubations ctenophores were removed and remaining copepods and carcasses were enumerated. An average of 83% (cydippid larvae incubations) and 41% (adult incubations) of the initial prey remained at the end of the incubation. Ctenophore clearance rates were calculated from the change in copepod or carcass abundance after correcting for losses of prey in predator-free controls (average of 14% live copepods and 18% carcasses lost in controls).

Carcass removal: Microbial decomposition—The decomposition of *A. tonsa* carcasses was observed through time at different temperatures and dissolved oxygen concentrations. To create carcasses at different stages of decomposition, fresh carcasses (CIV–CVI) were placed in Petri dishes (50 carcasses per dish) with 50 mL of 5-μm–filtered York River water and incubated at 5°C, 15°C, or 25°C on an orbital shaker table (30 rpm). Incubation containers were covered but not sealed so that normoxic treatments consisted of water at atmospheric equilibrium. To account for the influence of seasonal hypoxia in Chesapeake Bay (Diaz 2001), additional hypoxic and anoxic treatments were incubated at 25°C in a sealed incubation chamber (VWR model A-143) filled with specific gas mixtures (hypoxic gas: 3.8% O_2, 0.1% CO_2, balance N_2; anoxic gas: 2.5% H_2, balance CO_2). The water for the hypoxic and anoxic treatments was first bubbled for 10 min with the incubation gas; treated water was then measured into Petri dishes and copepod carcasses were added, taking care not to disturb and reoxygenate the water. Additional incubations were done for carcasses of naupliar and CI–CIII age classes at 15°C under normoxic conditions. Incubation lasted 30–120 h depending on incubation conditions, and triplicate Petri dishes from each treatment were removed at discrete times to measure carcass dry weight, abundance of carcass-associated bacteria, and carcass settling velocity (*see* next section) at different stages of decomposition.

Microbial decomposition of copepod carcasses was quantified as change in carcass dry weight and separately as change in carcass-associated bacterial abundance in the incubations described above. For dry weight measurements, carcasses (25–50 for copepodites; 75–150 for nauplii) were collected onto combusted pre-weighed GF/C filters, dried at 60°C for 24 h, and then weighed on a microbalance (Sartorius CPA2P-F; resolution 1 μg). For

bacterial abundances, measurements were taken only for adult female *A. tonsa* carcasses decomposing at 15°C normoxic conditions. These carcasses were rinsed briefly with sterile seawater and homogenized with a tissue grinder. The homogenates were filtered onto 0.2-μm black Nucleopore filters and stained with SYBR Gold™ (Chen et al. 2001), and stained bacteria were counted by epifluorescence microscopy (Bickel and Tang 2010).

Carcass removal: Hydrodynamic settling properties—Laboratory measurements were designed to provide estimates of carcass settling velocity, density, and equivalent spherical diameter (ESD). These hydrodynamic properties were estimated for carcasses at varying stages of decomposition from each age class of copepods (nauplii, CI–CIII, and CIV–CVI), as follows.

Carcass incubations for measurement of settling velocities were set up identically to those for dry weight and bacterial abundance measurements. Carcass settling velocities were measured in a transparent glass column (height, 21 cm; diameter, 2 cm) filled with ASW at 20°C. Individual carcasses at different stages of decomposition were gently released just beneath the water surface and were observed by eye (for copepodites) or using a video stereomicroscope (AMG model AMS-MV2; for nauplii). The carcasses were allowed to sink ~ 4 cm below the release point and were then timed as they passed five consecutive 1-cm intervals. The settling velocities of nine carcasses were observed for each discrete stage of decomposition and age class. Water-soluble red dye was used to check for thermal convection in the settling column. The dye was added at the column surface; it immediately sank to the bottom and then slowly and uniformly diffused upward. Once the dye had spread throughout the bottom half of the water column, the column was emptied and refilled with new ASW and dye. In some cases we observed rapid upward transport of dye or a non-uniform upward plume of dye. This was taken to indicate a convective current, and we discarded data from these trials. On several occasions carcasses were observed to slow their descent as they approached the glass column walls; therefore, data were also discarded if sinking carcasses came within several body lengths of a wall.

Fresh carcass density was measured using a variation of the density gradient method (Køgeler et al. 1987): Small flasks (50 mL) were filled with 10 fresh CIV–CVI carcasses and brine of various salinities (40–70 salinity) and temperatures (0–20°C). The flasks were mixed gently by inversion and allowed to sit for 10 min undisturbed. After 10 min, the number of carcasses that had sunk to the bottom was noted; we also noted those carcasses that were in suspension or floating near the surface. Carcasses that were neutrally buoyant (i.e., not sinking or floating) were considered to be of equal density to the solution containing them. The density of fresh nauplii and CI–CIII carcasses was assumed to be the same as that measured for CIV–CVI carcasses.

The gravitational settling velocity of a copepod carcass in water depends on the density and size (ESD) of the carcass as well as on the density and viscosity of the water. Carcass settling velocity measurements and fresh carcass density were used to estimate carcass ESD using a modified Stokes' Law for irregularly shaped particles (Ferguson and Church 2004), thus:

$$\omega_s = \frac{\mathrm{R}g\mathrm{D}^2}{\mathrm{C}_1 v + (0.75\mathrm{C}_2\mathrm{R}g\mathrm{D}^3)^{0.5}} \quad (1)$$

where ω_s is particle (carcass) settling velocity, R is submerged specific gravity $[(\rho_{\text{particle}} - \rho_{\text{fluid}})/\rho_{\text{fluid}}$, where ρ is density], g is gravitational acceleration, D is particle ESD, v is fluid kinematic viscosity, and C_1 and C_2 are constants (24 and 1.2, respectively; as recommended for angular grains by Ferguson and Church [2004]).

Measured values of fresh carcass density (ρ_{particle}) and settling velocity (ω_s) were applied in Eq. 1 to calculate fresh carcass ESD. Because the shape of the chitin carapace of a copepod carcass remains relatively intact for several days after death (Tang et al. 2006*a*,*b*), we assumed that carcass ESD was constant during decomposition. Therefore, ESD derived for fresh carcasses was applied to all other stages of decomposition, and measured carcass settling velocities were then used to estimate densities (ρ_{particle}) of the partially decomposed carcasses based on Eq. 1.

Effects of turbulence: Laboratory experiment—Average vertical current flow in the York River estuary is negligible compared to along-channel current velocity, as is true in most shallow systems (Pond and Pickard 1983). However, turbulent velocity fluctuations vertically mix the water column such that particles, including copepod carcasses, that have congregated at or near the benthos could be resuspended and mixed by upward turbulent diffusion. The Rouse model (Orton and Kineke 2001) approximates the vertical distribution of suspended particle concentration by assuming that turbulent diffusion and gravitational settling dominate transport and assuming that the turbulent eddy viscosity varies as a parabola with depth. If suspension follows the Rouse model, then the concentration of particles (C_z) at any height (z) above the bottom is given by

$$\mathrm{C}_z = \mathrm{C}_a \frac{\mathrm{z}(\mathrm{h}-\mathrm{z}_a)^{-\mathrm{Pr}}}{\mathrm{z}_a(\mathrm{h}-\mathrm{z})} \quad (2)$$

where C_a is particle concentration at a reference height (z_a) above the bottom, h is total water-column depth, and Pr is the Rouse parameter:

$$\mathrm{Pr} = \omega_s/\kappa \mathrm{u}_* \quad (3)$$

where ω_s is particle settling velocity, κ is von Kármán's constant (0.408), and u_* is shear velocity. The Pr indicates the relative importance of settling and turbulent fluxes, and values < 1 indicate that particle suspension is occurring throughout most of the water column (van Rijn 1993). Application of Eq. 2 to copepod carcasses in an estuary, however, requires extra caution because (1) settling velocity (ω_s) is not constant for carcasses at different stages of decomposition, (2) the assumption of parabolic eddy viscosity may be invalid when the water column is stratified, and (3) the vertical settling and diffusion terms may not be in balance, as is assumed in the Rouse model, as

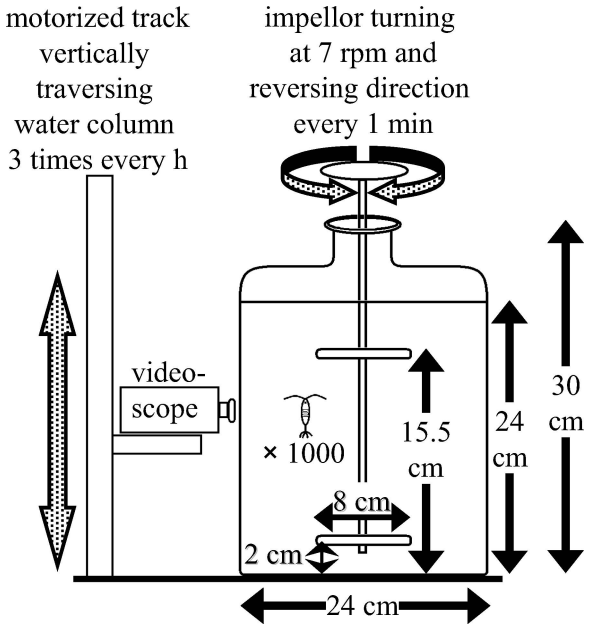

Fig. 1. Experimental setup for laboratory observation of vertical copepod carcass distribution throughout decomposition and under sustained turbulence.

a result of the production of new carcasses within the water column or horizontal advection.

A laboratory experiment was conducted to test whether Eq. 2 adequately described the vertical distribution of copepod carcasses in a closed and homogeneous system. A transparent 13-liter container (30 cm high, 24 cm in diameter) was filled to 24 cm in height with ASW at 20°C and continuously mixed by two 8-cm–long Teflon stir bars attached to an impellor shaft. Stir bars were fixed at 2 cm and 15.5 cm off the bottom and protruded 3.5 cm from either side of the impellor, which rotated at 7 rpm, reversing direction every minute (Fig. 1). This setup was based on that of Petersen et al. (1998) to simulate intermediate turbulent mixing conditions in the Choptank River, Chesapeake Bay. To begin the experiment, 1000 fresh *A. tonsa* (CIV–CVI) carcasses (~ 100 individuals L^{-1}) were added to the container. A video-stereomicroscope (AMG model AMS-MV2) attached to a motorized track slowly traversed the height of the water column three times per hour for 19 h, each time recording a profile of copepod carcass vertical distribution (56 profiles were recorded). Each recorded profile was analyzed by enumerating the carcasses within the microscope's field of view at 10 evenly spaced depths from 1 cm to 22.6 cm off the bottom. Equation 2 was fitted to these observations using non-linear least squares regression. C_z was set to the number of carcasses observed in the video-microscope field of view at each of the 10 depths, z_a was set to 2.18 cm off the bottom, and C_a was the mean number of carcasses observed at z_a. The Pr was estimated by fitting Eq. 2 to these data by the regression. For comparison, a simpler linear model was also fit to the vertical carcass distribution data.

Effects of turbulence: Field observations—A field study was conducted to evaluate the role that resuspension may play in determining the residence times of copepod carcasses in the water column and to test whether the Rouse model (Eq. 2) reasonably described the vertical distribution of copepod carcasses in the York River estuary. Copepod carcasses were sampled with a custom-built plankton pump at discrete depths at a single station in the York River (37.24°N, 76.50°W). This station was 9.1 m deep (± 0.4-m tidal range) and situated adjacent to a data buoy equipped with Acoustic Doppler Current Profiler (ADCP) for current velocity measurements (http://chsd.vims.edu/realtime/). The pump was housed in a watertight enclosure, and the water intake was fitted with a 63-μm mesh collection canister. Water was drawn directly into the canister such that the animals did not come into contact with the pump apparatus. The low flow rate of the pump (0.032 m^3 min^{-1}) was unlikely to cause mortality of copepods (Elliott and Tang 2009) but would likely undersample live copepods with escape jump behavior. However, our purpose was to sample carcasses; hence, potential undersampling of live copepods was not a concern. Samples were collected on 13 May 2009 from 08:00 h to 17:00 h Eastern Standard Time, spanning the majority of a tidal cycle (low tide ca. 06:55 h, high tide ca. 13:00 h, and subsequent low tide ca. 18:50 h). The pump was run for 5 min at a time followed by closure of the intake via a messenger. Samples were collected at shallow (2–3-m), intermediate (3–5-m), and deep (5–8-m) depths. A conductivity–temperature–depth profiler attached to the pump recorded the exact depth of each sample along with continuous temperature and salinity measurements. A total of 18 discrete depth samples were collected. To identify carcasses, collected samples were immediately stained with neutral red solution prior to preservation (Elliott and Tang 2009). Within each sample, carcasses of copepod nauplii and *A. tonsa* copepodite stages CI–CIII and CIV–CVI were enumerated, and all samples were processed within 10 d of collection. Each sample was counted in its entirety, and counts were converted to in situ carcass abundances. Samples containing a total of less than five carcasses were excluded from further analysis, since abundance estimates have very low precision when such low numbers are counted (Harris et al. 2000). Resulting data on vertical carcass distribution were fit with Eq. 2 by non-linear least squares regression, and the Pr (indicating the importance of resuspension) was estimated from the regressions.

Fate of carcass organic matter: Application to the York River estuary—To estimate the fate of copepod carcass organic matter in the York River estuary, all three removal mechanisms—necrophagy, sinking, and microbial decomposition—were combined in a simple mathematical model. This model represented the loss of carcass organic matter through time, beginning with 100 units of mass of fresh copepod carcass organic matter at mid-depth within the water column and proceeding until only the equivalent dry weight of the chitin carapace remained (assuming 8.35% of initial dry weight was chitin; Cauchie et al. 1997).

Table 1 shows the formulations and parameterization used in the mathematical model. Our experiments showed no statistically significant difference in ctenophore clear-

Table 1. Formulation, parameterization, and sources of data used in the model to predict the fate of copepod carcass organic matter in the York River estuary.

	Description	Value(s)	Units	Source (if applicable)
dCS/dt	Change in organic matter through time	$= -\text{CS} \times (a + b + c)$		
CS	Carcass dry weight pool	= 100	Units of mass	Assigned
a	Ctenophore population clearance rate	Winter = 0.020; spring = 0.089; summer = 0.015; fall = 0.026	h^{-1}	Purcell et al. 2001; Condon and Steinberg 2008
b	Rate of transfer from CS to microbial decomposition	$= (1 - \text{dry wt}_t / \text{dry wt}_{t-\Delta t})/\Delta t$	h^{-1}	
c	Rate of transfer from CS to benthos	$= \omega_{s(t)}/(0.5 \times \text{depth})$	h^{-1}	
dry wt_t	Carcass dry weight at time t after death	Variable	g copepod^{-1}	From Eq. 4
T	Water temperature	Winter = 5.5; spring = 18.0; summer = 26.3; fall = 15.4	°C	www.chesapeakebay.net/
DO	Dissolved oxygen condition	All seasons = 0; anoxic summer scenario = 1	None	
Δt	Time increment used	= 0.03125	h	Assigned
$\omega_{s(t)}$	Carcass settling velocity at time t after death	Variable	m h^{-1}	From Eqs. 1 and 5
depth	Channel depth of the York River estuary	= 10	m	Dellapenna et al. 1998

ance rates on live copepods vs. carcasses (*see* Results). We therefore estimated ctenophore population clearance rates on copepod carcasses from size-dependent individual *M. leidyi* clearance rate on live copepods (Purcell et al. 2001) and *M. leidyi* abundances and size distributions from the York River (Condon and Steinberg 2008). To account for the interplay between sinking and turbulent upward diffusion, two extreme scenarios for sinking losses were considered in the model. At one extreme, carcasses were assumed to remain suspended indefinitely (no sinking loss), and at the other extreme, carcasses were assumed to be removed immediately upon reaching the bottom (maximum sinking loss). The model was run separately for CIV–CVI, CI–CIII, and nauplii, for each season, for an additional anoxic summer scenario, and for both sinking loss scenarios.

Results

Carcass removal: Ctenophore selectivity—The presence or absence of stain had no significant effect on the ingestion of live copepods and carcasses by adult *M. leidyi*, regardless of which was stained (two-sample t-test, $t = 0.81$, df = 3, $p = 0.477$). Since ctenophores were not selective based on stain, live stained and dead stained treatments were combined for further analysis. The mean clearance rates by cydippid larvae on live copepods and carcasses were 0.03 and 0.07 L individual^{-1} h^{-1}, respectively. For adult ctenophores, the mean clearance rates were 0.61 and 0.64 L individual^{-1} h^{-1} on live copepods and carcasses, respectively. There were no significant differences in clearance rates for live copepods vs. carcasses (two-sample t-tests: for larvae, $t = -1.31$, df = 3, $p = 0.281$; for adults, $t = -0.16$, df = 9, $p = 0.875$).

Carcass removal: Microbial decomposition—Loss of carcass dry weight occurred most rapidly in the 25°C normoxic treatment, where dry weight dropped below the detection limit within 30 h (Table 2). CIV–CVI carcass dry weight decreased significantly and linearly with the logarithm of time since death ($R^2 = 0.547$; t-test, $t = -9.93$, df = 80, $p < 0.0005$). The dry weight of CI–CIII and naupliar carcasses at 15°C also decreased significantly and linearly with the logarithm of time since death (for CI–CIII, $R^2 = 0.396$; t-test, $t = -2.63$, df = 9, $p = 0.03$; for nauplii, $R^2 = 0.242$; t-test, $t = -2.20$, df = 12, $p = 0.05$). The rate of decrease of carcass dry weight was positively temperature dependent; that is, the slope of the linear regression line describing CIV–CVI carcass dry weight through time was significantly steeper for incubation at 25°C than at 5°C (t-test, $t = 2.98$, df = 35, $p < 0.05$). Though line slopes were not significantly different between normoxic and anoxic incubations (t-test, $t = 0.07$, df = 35, $p > 0.05$), dry weight did decrease more slowly in anoxic incubations (Table 2). Therefore, we included both dissolved oxygen and temperature as explanatory variables in a regression model describing carcass dry weight (dry wt) as a function of time, t, since death:

$$\text{dry wt}_t = \text{dry wt}_i + (\ln(t) + 1.39) \times \left[K_1 \times (1 - e^{k \times T}) + (K_2 \times DO)\right] \quad (4)$$

Table 2. Time series of copepod carcass dry weight (μg carcass^{-1}; mean with standard deviation in parentheses) through decomposition for different developmental stages, temperatures, and dissolved oxygen conditions; and carcass-associated bacterial abundance (bacterial cells carcass^{-1}) for CVI females decomposing at 15°C normoxic conditions ($n = 3$, except in cases denoted by *, where $n = 2$ because insufficient carcasses were recovered for a third measurement).

	Carcass dry weight							Bacterial abundance
	CIV–CVI					CI–CIII	Nauplii	CVI female
	5°C	15°C	25°C			15°C	15°C	15°C
Approximate time since death (h)	Normoxic	Normoxic	Normoxic	Hypoxic	Anoxic	Normoxic	Normoxic	Normoxic
0.25	3.6(1.3)	5(1.1)	2.7(1.0)	2.7(1.0)	4.9(0.7)	1(0.6)	0.2(0.0)*	37,800(25,300)
2			3.2(0.7)					
4			2.4(0.9)					
6					1.4(0.4)			
8	2(0.1)	2.6(0.6)		1.5(0.4)		0.6(0.2)	0.1(0.1)	38,300(4800)
10			1.4(0.9)		1.3(0.1)			
18	3.1(0.4)*	3.3(1.7)	0.1(0.4)				0.1(0.1)	36,800(7900)
24		3.5(0.5)			1.5(0.5)	0.5(0.3)*		89,400(55,600)
30	2.4(0.8)		0				0.1(0.1)*	
48	2.5(1.1)*	2(0.4)		0.1(0.4)	0.9(0.4)	0.2(0.2)	0.1(0.1)	53,000(6600)
72		1.9(0.3)			0.4(0.2)			94,100(41,000)
96								104,700(10,900)
116	1.8(0.4)							

where dry wt_t is carcass dry weight (μg carcass^{-1}) at time t after death (from 0.25 h onward), dry wt_i is initial carcass dry weight, T is water temperature (°C), DO is an indicator variable (0 = normoxic; 1 = hypoxic or anoxic), and K_1, K_2, and k are constants that were estimated by the non-linear regression using an iterative approach. Equation 4 predicts dry wt_t to decrease linearly with ln(t), with the rate of decrease (slope) determined as a linear function of dissolved oxygen condition and an exponential saturation function of temperature. The parameter estimates that resulted in the best fit of Eq. 4 to CIV–CVI carcass dry weight data were dry $wt_i = 4.178$ μg carcass^{-1}, $K_1 = -4.166$, $K_2 = 0.046$, and $k = -0.008$°C^{-1}. The resulting model fit the data with $R^2 = 0.631$.

The mean initial bacterial abundance associated with adult female carcasses was 3.78×10^4 carcass^{-1}. Changes in the abundance of carcass-associated bacteria did not coincide with changes in carcass dry weight, as indicated by the lack of a significant correlation between the averages of these two metrics (Pearson correlation, $r = -0.577$, $t = -1.41$, df = 4, $p = 0.231$). For example, maximum dry weight loss occurred in the first 8 h after death, during which time bacterial abundance remained nearly constant (Table 2).

Carcass removal: Hydrodynamic settling properties—Copepod carcass settling velocity decreased rapidly in the first several hours after death, and more slowly thereafter (Table 3). Mean fresh carcass density was 1049 kg m^{-3} ($\pm$ 0.3 kg m^{-3}; 95% confidence interval) and was combined with fresh carcass settling velocity (mean of Table 3 initial values; $\omega_s = 0.125$, 0.08, and 0.03 cm s^{-1} for CIV–CVI, CI–CIII, and nauplii, respectively) to calculate ESD using Eq. 1 ($\rho_{fluid} = 1013$ kg m^{-3} and $\nu = 1.0 \times 10^{-6}$ m^2 s^{-1}). The resulting ESDs were 333 μm for CIV–CVI, 243 μm for CI–CIII, and 141 μm for nauplii. Using these ESDs and measured carcass settling velocities (Table 3) in Eq. 1, carcass densities were calculated at different stages of decomposition. Resulting densities of carcasses of both copepodite groups decreased significantly and linearly with the natural logarithm of time (Fig. 2 for CIV–CVI, $R^2 = 0.378$; t-test, $t = -23.87$, df = 936, $p < 0.0005$; for CI–CIII, $R^2 = 0.099$; t-test, $t = -3.87$, df = 128, $p < 0.0005$), but not significantly for nauplii ($R^2 = 0.007$; t-test, $t = 1.13$, df = 40, $p = 0.264$). As was the case with dry weight, the rate of decrease of carcass density was positively temperature dependent, with a linear regression line describing decrease in CIV–CVI carcass density through time that was significantly steeper at 25°C than at 5°C (two-sample t-test, $t = 2.1$, df = 413, $p < 0.05$). Although line slopes did not significantly differ between normoxic and anoxic incubations (two-sample t-test, $t = 0.02$, df = 389, $p > 0.05$), carcass density did decrease more slowly in anoxic incubations (Fig. 2 for CIV–CVI). Therefore, we included both temperature and oxygen as explanatory variables in a regression model describing carcass density (ρ) as a function of time t since death:

$$\rho_t = \rho_i + (\ln(t) + 1.39) \times \left[K_1 \times (1 - e^{k \times T}) + (K_2 \times DO)\right] \quad (5)$$

Equation 5 is analogous to Eq. 4, where ρ_t is predicted carcass density (kg m^{-3}) at time t after death (from 0.25 h onward). Parameter estimates for CIV–CVI carcasses from non-linear regression using an iterative approach were ρ_i (initial carcass density) = 1045 kg m^{-3}, $K_1 = -3.78$, $K_2 = 0.731$, and $k = -0.329$°C^{-1}. The resulting model fit the data with $R^2 = 0.398$. Model predictions of carcass density from Eq. 5 are shown as lines in Fig. 2.

Settling velocities predicted from Eqs. 1 and 5 were, on average, 23% higher than our empirical measurements (Table 3), indicating that carcass ESD may have decreased slightly during decomposition. To account for this, predicted settling velocities were adjusted by a factor of

Table 3. Time series of copepod carcass settling velocity (cm s^{-1}; mean with standard deviation in parentheses) through decomposition for different developmental stages, temperatures, and dissolved oxygen conditions (n = 24–40 for copepodites and 7–9 for nauplii).

Approximate time since death (h)	CIV–CVI					CI–CIII		Nauplii
	5°C	15°C	25°C			15°C		15°C
	Normoxic	Normoxic	Normoxic	Hypoxic	Anoxic	Normoxic		Normoxic
0.25	0.120(0.032)	0.124(0.023)	0.120(0.032)	0.120(0.032)	0.129(0.039)	0.078(0.043)		0.027(0.010)
2	.	.	0.106(0.015)	.	.	.		.
4	.	0.078(0.026)	0.076(0.020)	.	.	.		.
6	.	.	.	.	0.099(0.058)	.		.
8	0.089(0.021)	0.070(0.025)	.	0.097(0.025)	.	0.081(0.024)		0.044(0.021)
10	.	.	0.069(0.025)	.	0.085(0.038)	.		.
18	0.057(0.021)	0.061(0.022)	0.066(0.022)	0.070(0.032)	.	0.063(0.032)		0.025(0.007)
24	.	0.066(0.021)	.	.	0.081(0.044)	.		.
30	0.075(0.022)	.	0.060(0.029)	.	.	.		0.030(0.009)
48	0.085(0.027)	0.047(0.017)	.	0.057(0.012)	0.050(0.022)	0.041(0.018)		0.049(0.033)
72	.	.	.	.	0.056(0.028)	.		.
116	0.060(0.024)	.	.	.	.	.		.

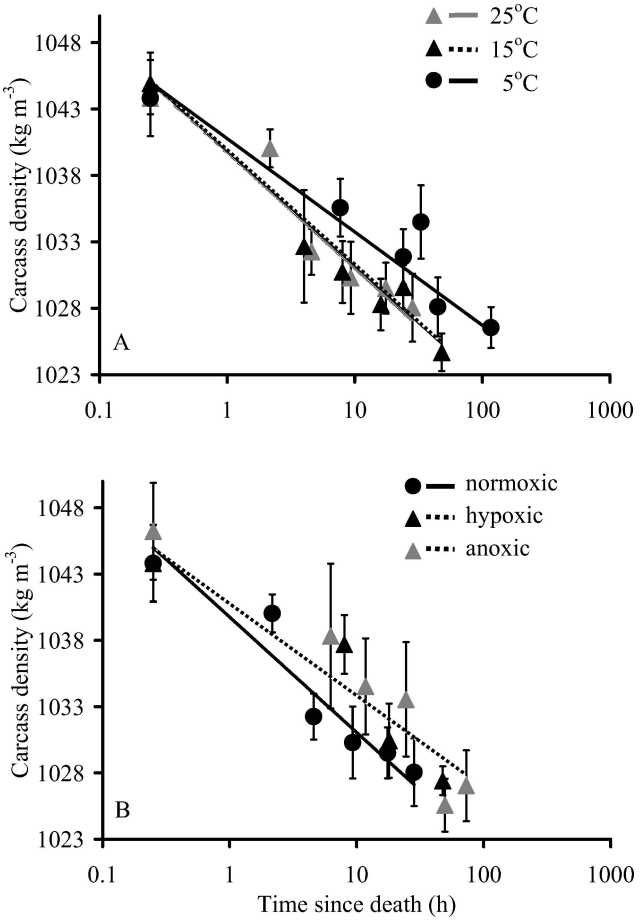

Fig. 2. Mean density (symbols; derived from measured settling velocity) and predicted density (lines; derived from Eq. 5) for CIV–CVI copepod carcasses decomposing under different (A) temperatures and (B) dissolved oxygen conditions. Error bars are 95% confidence intervals. X-axes log-scale.

1/1.23. The adjusted predictions agreed closely with observations for copepodites and nauplii (Fig. 3; R^2 = 0.733; t-test of regression slope, t = 10.0, df = 36, $p <$ 0.0005), and this adjustment was subsequently made to predicted settling velocities used in the Rouse model (Eq. 2) and in the mathematical model predicting the fate of carcass organic matter (Table 1).

Effects of turbulence: Laboratory experiment—Copepod carcass abundance increased with depth in all 56 recorded profiles (Fig. 4). The linear regression model described vertical carcass distribution quite well (t-test, t = 21.28; df = 513; $p < 0.0005$; R^2 = 0.42), but the Rouse model (Eq. 2) provided a slightly better fit to the data (R^2 = 0.48). The estimated 95% confidence interval of the Pr was 0.36–0.42, corresponding to a shear velocity (u_*) of $\sim$ 0.5 cm s^{-1} based on an intermediate ω_s of 0.085 cm s^{-1}, chosen to be representative of the 19-h experimental period.

Effects of turbulence: Field observations—Copepodite carcass abundance increased with depth in the York River (Fig. 5A,B). The Rouse model (Eq. 2) was fit to these

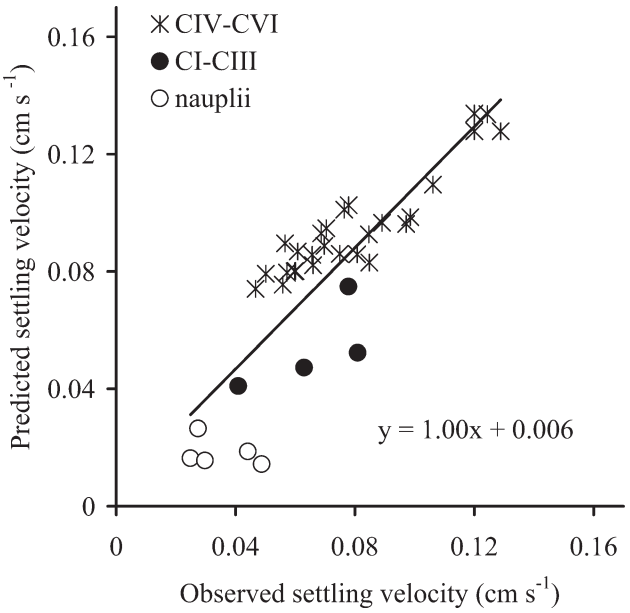

Fig. 3. Relationship between measured copepod carcass settling velocities and those predicted for the same carcasses using Eqs. 1 and 5 and the adjustment factor (0.81).

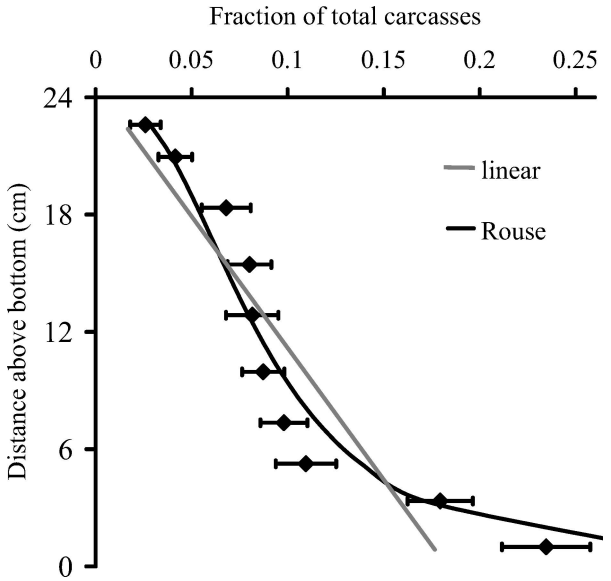

Fig. 4. Observed profile of the vertical distribution of CIV–CVI copepod carcasses from the laboratory turbulence experiment. Values are means (averaged across all 56 profiles) of the fraction of the observed carcasses that occurred at each depth interval in the experimental container. Error bars are 95% confidence intervals. Also shown are estimates made using the Rouse and linear regression models fit to these data.

abundances, resulting in characteristic profiles over the sampling period (Fig. 5, Rouse prediction). The regression was not attempted for naupliar carcasses, the abundance of which did not vary with depth (Fig. 5C). Reference height (z_a) in these regressions was set as 6.1 m above bottom (3 m in depth), where we had the most replicate samples and likely the highest accuracy in measured concentrations. Reference concentration (C_a) was set to the mean carcass abundance at z_a. There was a strong relationship between observed copepodite carcass abundance and Eq. 2 predictions ($R^2 = 0.725$ for CIV–CVI; $R^2 = 0.809$ for CI–CIII). The estimated 95% confidence intervals for Pr were 0.29–0.52 for CIV–CVI and 0.44–0.68 for CI–CIII, indicating that resuspension of carcasses was important, as was gravitational settling ($Pr < 1$). Assuming settling velocities of intermediate-aged carcasses (18 h, Table 3, ω_s = 0.06 cm s^{-1} for both CIV–CVI and CI–CIII) these Rouse parameters corresponded to a shear velocity of $\sim$ 0.2–0.5 cm s^{-1} (95% confidence intervals: 0.28–0.51 cm s^{-1} for CIV–CVI, and 0.22–0.33 cm s^{-1} for CI–CIII).

Fate of carcass organic matter: Application to the York River estuary—Model estimates of carcass fate were expressed as percentages of carcass organic matter removed by the three different mechanisms (Table 4). The model was run under two different assumptions of sinking losses to consider the implications of turbulence. The first assumed no resuspension (maximum sinking losses), and the second assumed that resuspension retained carcasses in the water column indefinitely (no sinking losses).

When maximum sinking loss was considered, the time required for removal of all copepod carcass organic matter was 3–4 h for CIV–CVI, 5–7 h for CI–CIII, and 11–20 h for nauplii (Table 4). Sinking was the dominant removal mechanism, although it was relatively less important for nauplii because of their lower settling velocities. Microbial decomposition removed much of the remainder of carcass organic matter (7–30% for CIV–CVI, 9–39% for CI–CIII, and 12–57% for nauplii), and its importance varied seasonally based on water temperature and competition with necrophagy. Compared to decomposition and sinking, necrophagy by ctenophores removed a small amount of carcass organic matter (2–6% for copepodites and 6–14% for nauplii), except in the spring, when ctenophore population clearance rate was highest (Table 1). Seasonal anoxia caused only a slight decrease in losses to microbial decomposition and a slight increase in sinking losses (2–5%), but no change in losses to necrophagy (Table 4).

At the other extreme, when the model neglected sinking losses, it took 19–111 h for carcass organic matter to be removed (Table 4). These results applied to all developmental stage groups since the same rates of dry weight loss and ctenophore clearance were applied to all stages. In the absence of sinking, the importance of ctenophore ingestion (necrophagy) became disproportionately larger, and was comparable to microbial decomposition in removing copepod carcasses (Table 4).

Discussion

In this section we summarize our findings on carcass removal via necrophagy, microbial decomposition, and gravitational settling in the presence of turbulence, and we compare our results to those of other studies. Then we synthesize our findings into a general representation of the fate of copepod carcass organic matter in the York River estuary. Finally, we discuss the ecological implications in

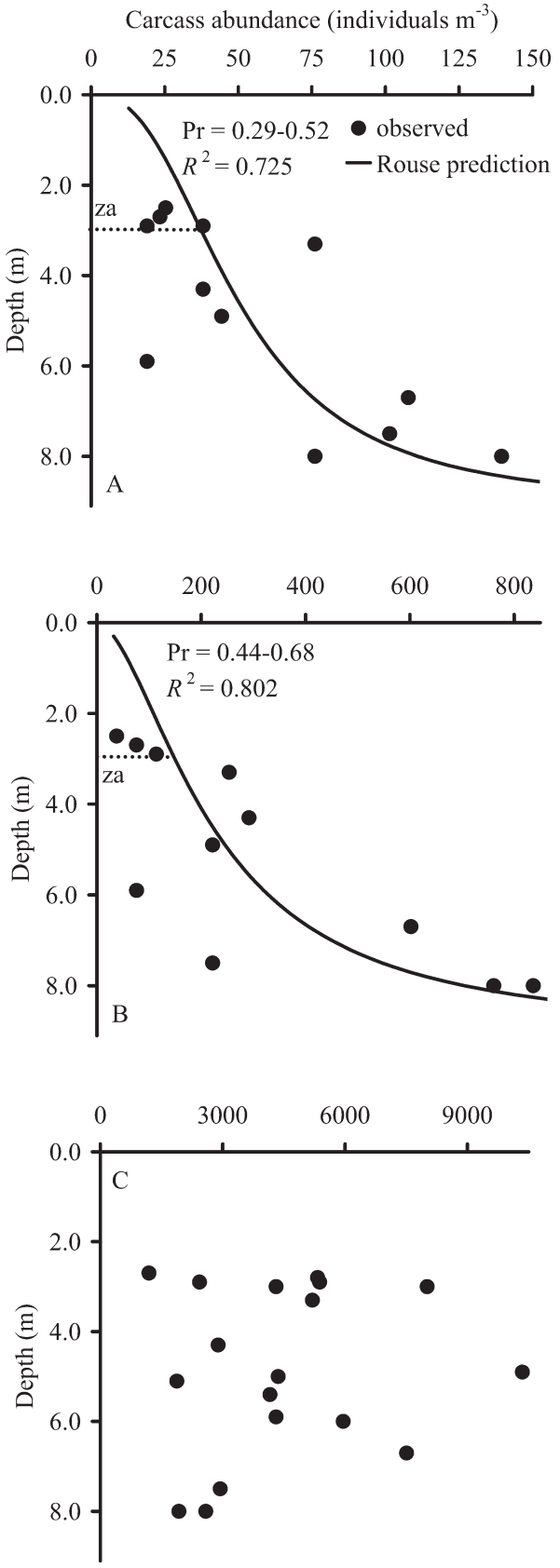

Fig. 5. Vertical copepod carcass distribution in the York River estuary for (A) CIV–VI, (B) CI–CIII, and (C) nauplii. Black circles represent observed carcass abundances (from pump samples); lines are best fits of Eq. 2 (Rouse model). No regression solution was attempted for nauplii. Pr is the estimated 95% confidence interval of the Rouse parameter derived from the regressions, and z_a is the reference depth used in Eq. 2. Note different scales for x-axes.

estuaries such as the York River and in the larger marine environment.

Carcass removal: Ctenophore selectivity—We found that ctenophores did not strongly select for live copepods or carcasses, consuming each in similar proportion to their abundance in the water. Several studies (Purcell et al. 1991; Costello et al. 1999; Waggett and Costello 1999) have shown particle selectivity by ctenophores and other gelatinous planktivores. However, in our bottle incubations, selectivity between live copepods and carcasses was not detected. Ctenophores are not the only York River planktivore that may ingest copepods and their carcasses. However, *M. leidyi* is both abundant and persistent in the York River (Steinberg and Condon 2009) and represents the dominant predator on mesozooplankton in Chesapeake Bay (Baird and Ulanowicz 1989). Therefore, as a first approximation we assumed that both live copepods and carcasses were cleared at the same rate in the field and that this clearance rate was set by *M. leidyi* abundance and size distribution.

Carcass removal: Microbial decomposition—Following death, the dry weight (and density) of copepod carcasses decreased rapidly at first and more slowly as time progressed. This log-linear type of trajectory of decomposition has been found in other studies of zooplankton carcass decomposition (Seiwell and Seiwell 1938; Lee and Fisher 1994; Bickel and Tang 2010) and also specifically for the decomposition of detritus (Jenny et al. 1949; Olson 1963; Wider and Lang 1982). Overall, the regression models (Eqs. 4 and 5) performed well in terms of describing carcass decomposition (dry weight and density losses) through time and for different temperature and dissolved oxygen conditions (R^2 describing 40–63% of variation). Some of the unexplained variation may have been due to grouping of multiple developmental stages. Size differences can be large among developmental stages of *A. tonsa*, and carcass settling velocity and dry weight will vary accordingly. For example, the dry weight of CIV *A. tonsa* is approximately half that of CVI, and length of CIV is approximately 2/3 that of CVI (Heinle 1966). Although individual copepods were selected randomly for experiments, variation around the mean of measured dry weight and settling velocity could have been magnified by a disproportionately large number of individuals of a single developmental stage within specific replicates.

The abundance of bacteria associated with copepod carcasses (Table 2) was comparable that described in reports of naturally occurring Chesapeake Bay calanoid copepods (0.3–9.6 $\times$ 10^5 cells carcass^{-1}; Heidelberg et al.

Table 4. Predictions resulting from the carcass fate model (Table 1), including % of total organic matter removed by each mechanism and model run time (time for all carcass organic matter except chitin to be removed). For the maximum sinking loss scenario, separate predictions are shown for each developmental stage group and season (ANX = anoxic). Predictions for the no-sinking loss scenario apply to all developmental stages.

Developmental stage	Season scenario	Microbial decomposition (%)	Necrophagy (%)	Sinking (%)	Model run time (h)
CIV–CV: sinking	Winter	7	3	90	4
	Spring	20	10	70	3
	Summer	30	2	68	3
	Summer ANX	28	2	70	3
	Fall	18	4	78	4
CI–CIII: sinking	Winter	9	5	86	7
	Spring	26	16	58	5
	Summer	39	3	58	5
	Summer ANX	36	3	61	5
	Fall	24	6	70	7
Nauplii: sinking	Winter	12	14	74	20
	Spring	34	31	35	10
	Summer	57	6	37	11
	Summer ANX	52	6	42	12
	Fall	34	14	52	16
All stages: no sinking	Winter	20	80	NA	111
	Spring	44	56	NA	19
	Summer	88	12	NA	26
	Summer ANX	86	14	NA	33
	Fall	51	49	NA	58

2002) and laboratory *A. tonsa* cultures (10^3–10^5 cells carcass^{-1}; Tang 2005). Maximum dry weight loss occurred in the first 8 h after death, but bacterial abundance remained nearly constant until 16 h after death. This initial 8–16-h period may represent a lag phase in the growth of bacteria decomposing the carcasses, during which time the bacteria actively produced exoenzymes to break down copepod tissues, but bacterial population growth was still slow (Bickel and Tang 2010). Assuming a bacterial cell diameter of 1.0 μm, a volume-to-carbon conversion of 0.09 $\times$ volume$^{0.6}$ (Norland 1993), and a carbon content of 50% of dry weight (Norland 1993), the observed maximum carcass associated bacterial abundance (104,700 cells carcass^{-1}) corresponded to a dry weight of < 0.13 μg, or $< 7\%$ of total carcass dry weight. Hence, carcass-associated bacteria contributed a negligible fraction to the total carcass dry weight.

Carcass removal: Hydrodynamic settling properties—The gravitational settling velocity of a copepod carcass in water depends on the density and size (ESD) of the carcass and the density and viscosity of the water, as described in Eq. 1. Measured settling velocity, density, and ESD of carcasses agreed well with values found in the literature. Our measurements of copepodite carcass settling velocities (ca. 0.1 cm s^{-1}, Table 3) were comparable to reports for passively sinking live *A. tonsa* (0.08 $\pm$ 0.021 cm s^{-1}; Jonsson and Tiselius 1990). The density of fresh *A. tonsa* carcasses (1049 $\pm$ 0.3 kg m^{-3}, 95% confidence interval) was slightly higher than that reported for *Calanus finmarchicus* (1027–1045 kg m^{-3}; Knutsen et al. 2001) and *Acartia clausii* (1045 kg m^{-3}; Greenlaw 1977). ESDs estimated from settling velocities and density (333 μm, 243 μm, and 141 μm for CIV–CVI, CI–CIII, and nauplii, respectively) compared well with independent estimates based on *A. tonsa* body volume (from Mauchline 1998) and assuming cylindrical (copepodites) and spherical (nauplii) shapes (345 μm, 199 μm, and 125 μm for CIV–CVI, CI–CIII, and nauplii, respectively). In our ESD calculations we assumed that the densities of CI–CIII and copepod nauplii were identical to that measured for CIV–CVI. Although the assumption is reasonable among copepodite stages, the density of nauplii may be slightly higher, since lipids tend to contribute slightly less to total naupliar dry weight (van der Meeren et al. 2008). However, this difference is likely unimportant given the already low settling velocity of nauplii. For example, if instead we assume a density of 1071 kg m^{-3} (maximum reported *Acartia* spp. density; Mauchline 1998), the difference in settling velocity predicted by Eq. 1 is small (< 0.017 cm s^{-1}) and is within the range of variability of naupliar settling velocity measurements (Table 3).

Effects of turbulence—A goal of the turbulence experiments was to verify that carcasses behaved as passive sinking particles throughout decomposition, which was substantiated by the observation that carcass concentration increased significantly with depth throughout decomposition in the laboratory (Fig. 4). A second purpose of these experiments was to evaluate the ability of the Rouse model (Eq. 2) to accurately describe the vertical distribution of copepod carcasses and, thereby, to provide a way to quantify the relative importance of vertical mixing and gravitational settling to the fate of copepod carcasses. The Rouse model described the vertical distribution of carcasses fairly well in the laboratory (Fig. 4) and in the field (Fig. 5A,B). The Rouse parameter Pr (Eq. 3) was useful for capturing the curvilinear shape of carcass distribution with depth (Figs. 4, 5A,B), which could not be done with the

linear model (Fig. 4). The linear model also had the undesirable potential of predicting negative carcass abundances at shallow depths (negative y-intercept possible). Finally, the linear model required estimation of both line slope and intercept, while the Rouse model required estimation only of the Pr. We concluded that the Rouse model (Eq. 2) described carcass profiles better than the linear model, supporting its use to describe the vertical distribution of copepod carcasses.

As a means of further assessment, estimates of u_* from the regressions of the Rouse model to carcass abundances in the field (Fig. 5A,B) were compared to independent field-derived u_* estimates from the quadratic stress law (Orton and Kineke 2001) and using ADCP current speed data (1.12 m above the bottom). A typical drag coefficient of 0.0015 for the central portion of the York River was assumed (Scully and Friedrichs 2003). Estimates of u_* from the quadratic stress law ranged from 0.06 to 2.04 cm s^{-1}, with a time average of 0.82 cm s^{-1}, slightly higher than estimates based on vertical carcass distribution measurements in the field ($\sim$ 0.2–0.5 cm s^{-1}). This discrepancy was not surprising, given the tendency for thermohaline- and sediment-induced stratification to reduce turbulent stresses and apparent shear velocity in the mid–water column of the York River (Friedrichs et al. 2000). As is typical of this estuary, strong thermohaline stratification was present during our field sampling. The change in water density from 2.5–8-m depth (the range of sample collection) was 0.9 kg m^{-3}, and this may explain the lower shear velocities estimated from observed carcass distribution.

Fate of carcass organic matter in the York River estuary—The predicted fate of carcass organic matter depended heavily on the magnitude of sinking losses (Table 4). Assuming a settling velocity of $\sim$ 0.1 cm s^{-1} (Table 3) and an average channel depth of $\sim$ 10 m (Dellapenna et al. 1998), copepodite carcasses could sink out of the York River water column in under 3 h. However, several lines of evidence indicate that most carcasses remain in the water column for much longer as a result of turbulent mixing: (1) Tang et al. (2006*a*) observed that an average 29% of collected copepods were carcasses in the York River during summer 2005. In the absence of resuspension and upward turbulent diffusion, the high carcass abundance and high settling velocity translate to an extremely high post-hatch mortality rate of ca. 2.32 d^{-1}. This far exceeds the estimated population growth rate ($\leq$ 0.73 d^{-1}) for the summer, when copepod abundance is increasing (D.T. Elliott unpubl.). Thus, a more reasonable explanation is that vertical mixing helps retain carcasses in the water column. (2) Our laboratory experiment showed that copepod carcasses could be suspended throughout the water column by turbulence and that concentrations increased with depth (Fig. 4). (3) Our field data confirmed that copepod carcasses were found throughout the water column, with abundances increasing with depth (Fig. 5A,B). The Pr estimated from field abundances of copepodites was well below 1.0 (Fig. 5A,B), indicating that turbulent resuspension was occurring throughout much of the water column (van Rijn 1993). (4) Turbulent resuspension will be important for particles having a Pr of < 1.0 (van Rijn 1993). The time-averaged shear velocity from ADCP data ($u_* = 0.82$ cm s^{-1}) corresponds to a Pr below 1.0 for particles with settling velocities < 0.3 cm s^{-1}. Our empirically derived settling velocities were all lower than this threshold (Table 3).

Thus, carcasses within the York River do sink but may congregate near the bottom, where turbulent mixing is most intense. Some of the carcasses will be deposited to the bed, especially during periods of low turbulence, such as at slack tide. These, however, may be subsequently resuspended and mixed into the overlying water column, especially when tidal currents and turbulent mixing increase. The true budget for the fates of copepod carcasses lies somewhere between the two extreme scenarios of zero and maximum sinking losses.

The influence of horizontal advection on carcass distribution should be analogous to that of suspended sediments of a similar settling velocity. Suspended sediments in the York River estuary often converge within one of two turbidity maxima, both located $>$ 20 km upstream of the estuary's mouth (Friedrichs 2009). At a maximum carcass residence time of 111 h (Table 4) and a 7 cm s^{-1} net landward flow as a result of estuarine circulation (Friedrichs 2009), a carcass could be transported 28 km upstream, approximately half the length of the estuary. Hence, the overall effect of horizontal advection would be to retain carcasses within the estuary and possibly to concentrate them in the estuarine turbidity maxima. This would be especially important when carcass residence time is long, as is the case in the winter (Table 4). Elevated copepod abundances have been observed in estuarine turbidity maximum regions (Morgan et al. 1997; Roman et al. 2001), and our results indicate that this phenomenon could partially result from passive concentration of carcasses there. In this case, one would expect to find high relative abundances of carcasses in zooplankton samples taken from turbidity maximum regions.

Broader ecological implications—Based on this and other studies, it is clear that microbial decomposition of copepod carcasses represents an alternative trophic pathway for zooplankton secondary production. The importance of carcass organic matter to microbial production in the York River estuary can be estimated as follows: Bacterial carbon demand (BCD) for the York River is estimated to be 0.8–4.2 mg C m^{-3} h^{-1} (Schultz [1999], for a 10-m–deep water column). Assuming a copepod production of 0.24 mg C m^{-3} h^{-1} (Purcell et al. [1994], mesohaline portion of the Chesapeake Bay) and an instantaneous nonpredatory mortality rate of $\sim$ 0.1 d^{-1} for copepods (Mauchline 1998; Tang et al. 2006*a*), we estimate a rate of 0.024 mg C m^{-3} h^{-1} for the conversion of copepod production to carcasses. If 58% of this is directly utilized by bacteria (average of no-sinking scenario; Table 4), then carcass decomposition will be equivalent to consumption of 0.014 mg C m^{-3} h^{-1} by microbes, or 0.3–1.8% of York River BCD. This estimate is substantially higher than that noted by Tang et al. (2006*a*) for the summer of 2005, likely because it considers all copepod developmental stages

(rather than just adults) and includes springtime copepod production, which can be higher than that in the summer.

We can make a similar calculation of the potential contribution of carcasses to water-column particulate organic carbon (POC) and POC flux to the benthos. Total POC in York River surface water is on the order of 1–2 mg C L^{-1} (Countway et al. 2003). Assuming a maximum carcass residence time of 111 h in the water column (Table 4), the estimated average production of copepod carcass organic matter (0.024 mg C m^{-3} h^{-1}, *see* above) corresponds to a carcass carbon concentration of 2.7 μg C L^{-1}. This indicates that copepod carcasses represent $< 0.3\%$ of York River water-column POC. Flux of POC to the benthos has been estimated as 20.6–42.5 mg C m^{-2} h^{-1} annually in the mesohaline portion of Chesapeake Bay (Roden et al. 1995). Assuming an 0.24 mg C m^{-2} h^{-1} carcass organic matter production rate (0.024 mg C m^{-3} h^{-1} for a 10-m–deep water column, *see* above) and 63% sinking losses (average of sinking scenarios; Table 4), copepod carcasses could account for 0.4–0.7% of organic matter deposited to the York River bottom.

These estimates indicate that copepod carcasses likely contribute only small fractions to the total York River BCD, water-column POC, and POC flux to the benthos. Nevertheless, carcasses provide important localized hot spots of microbial growth and activity that may select for specific bacterial phylotypes and, hence, affect microbial diversity in the water column (Tang et al. 2006*b*, 2009). Carcasses are also labile particulate organic matters that could be a nutritious food source for benthic fauna (Zajączkowski and Legeżyńska 2001).

Our results also have implications for the fate of copepod carcasses in other environments. Considering an oceanic copepod species with initial carcass density and rate of density reduction that are identical to those measured for *A. tonsa*, a carcass decomposing in the relatively warm surface ocean (at 15–25°C) would approach a density of 1028 kg m^{-3} after 24–48 h (Fig. 2A). At this time it would be approximately neutrally buoyant with the water below the permanent thermocline ($\sigma_t \sim 28$). Using Eqs. 1 and 5, we predicted sinking trajectories through time of a copepod carcass (prosome length 2000 μm, ESD 1028 μm) in freshwater (0 salinity), mesohaline water (18 salinity), and seawater (35 salinity), at temperatures of 5°C, 15°C, and 25°C and in the absence of net vertical water movement. The effect of temperature on predicted trajectory was moderate. Carcass density decreased more slowly in cold water (5°C), but the carcass also sank more slowly, since cold water is denser. Conversely, in warm water (25°C), carcass density decreased more rapidly, but the carcass also sank faster. The effect of salinity was more pronounced. Relative to freshwater, predicted settling velocity decreased markedly in mesohaline water as the carcass decomposed and became less dense. However, the effect of decreasing carcass density was most notable in seawater, where the carcass was predicted to achieve neutral buoyancy between 40 and 77 h after death, during which time it would have sunk approximately 150–300 m. Assuming instead a water temperature of 0°C at the depth of neutral buoyancy, carcasses at this depth would decompose slowly enough to remain relatively intact for weeks. This may explain the congregations of zooplankton carcasses observed at or below the permanent thermocline in several oceanic studies (Terazaki and Wada 1988; Geptner et al. 1990; Böttger-Schnack 1996).

Using a combined experimental, observational, and modeling approach, this study quantified the relative importance of necrophagy, microbial decomposition, and sinking to removal of copepod carcass organic matter. We found that turbulent mixing in shallow tidal systems can keep carcasses in suspension much longer than gravitational settling alone would imply. Therefore, a large portion of copepod carcass organic matter may fuel microbial and necrophage production in the water column, as predicted in the model scenario that excluded sinking losses (Table 4). This may also occur in the open ocean as a result of the large distances that a carcass must sink and the potential for a carcass to achieve neutral buoyancy.

The importance of the removal of carcasses that are near the bed by ingestion by benthic fauna in shallow systems is not presently clear, nor is the importance of carcass incorporation into sinking aggregates or burial in bed sediments. Further work on carcass sinking losses should focus on resolving the balance between gravitational settling and upward turbulent diffusion, perhaps using a hydrodynamic model coupled with observations of carcass abundance close to and on the seabed. The results of this study highlight the importance of considering live and dead composition in zooplankton sampling and pelagic food web models, given that carcasses can remain in the water column for extended periods of time.

Acknowledgments

We thank M. A. Lynch and C. S. Freund for technical assistance, P. J. Dickhudt for advice on York River physics, and M. J. Brush, M. R. Roman, and three anonymous reviewers for critical reviews of earlier drafts. S. L. Bickel also provided the bacterial abundance data and C. T. Friedrichs the ADCP data. This research was funded by U.S. National Science Foundation (NSF) Ocean Sciences 0814558, awarded to K.W.T. D.T.E. also received financial support from NSF GK-12 (Division of Graduate Education 0840804, awarded to K.W.T.). This article is Contribution 3092 of the Virginia Institute of Marine Science, College of William and Mary.

References

Baird, D., and R. E. Ulanowicz. 1989. The seasonal dynamics of the Chesapeake Bay ecosystem. Ecol. Monogr. **59:** 329–364, doi:10.2307/1943071

Bickel, S. L., and K. W. Tang. 2010. Microbial decomposition of proteins and lipids in copepod versus rotifer carcasses. Mar. Biol. **157:** 1613–1624, doi:10.1007/s00227-010-1434-4

Böttger-Schnack, R. 1996. Vertical structure of small metazoan plankton, especially noncalanoid copepods. I. Deep Arabian Sea. J. Plankton Res. **18:** 1073–1101, doi:10.1093/plankt/18.7.1073

Cauchie, H. M., G. Murugan, J. P. Thomé, and H. J. Dumont. 1997. Intra- and interspecific variations in the chitin content of some anostracans. Hydrobiologia **359:** 223–228, doi:10.1023/A:1003110803360

Chen, F., J. R. Lu, B. J. Binder, Y. C. Liu, and R. E. Hodson. 2001. Application of digital image analysis and flow cytometry to enumerate marine viruses stained with SYBR Gold. Appl. Environ. Microbiol. **67:** 539–545, doi:10.1128/AEM.67.2.539-545.2001

Condon, R. H., and D. K. Steinberg. 2008. Development, biological regulation, and fate of ctenophore blooms in the York River estuary, Chesapeake Bay. Mar. Ecol. Prog. Ser. **369:** 153–168, doi:10.3354/meps07595

Costello, J. H., R. Loftus, and R. Waggett. 1999. Influence of prey detection on capture success for the ctenophore *Mnemiopsis leidyi* feeding upon adult *Acartia tonsa* and *Oithona colcarva*. Mar. Biol. **191:** 207–216.

Countway, R. E., R. M. Dickhut, and E. A. Canuel. 2003. Polycyclic aromatic hydrocarbon distributions and associations with organic matter in surface waters of the York River, VA estuary. Org. Geochem. **34:** 209–224, doi:10.1016/S0146-6380(02)00162-6

Dellapenna, T. M., S. A. Kuehl, and L. C. Schaffner. 1998. Sea-bed mixing and particle residence times in biologically and physically dominated estuarine systems: A comparison of lower Chesapeake Bay and the York River estuary. Estuar. Coast. Shelf Sci. **4:** 777–795, doi:10.1006/ecss.1997.0316

Diaz, R. J. 2001. Overview of hypoxia around the world. J. Environ. Qual. **30:** 275–281.

Dubovskaya, O., M. Gladyshev, V. G. Gubanov, and O. N. Makhutova. 2003. Study of non-consumptive mortality of crustacean zooplankton in a Siberian reservoir using staining for live/dead sorting and sediment traps. Hydrobiologia **504:** 223–227, doi:10.1023/B:HYDR.0000008522.88010.45

Elliott, D. T., and K. W. Tang. 2009. Simple staining method for differentiating live and dead marine zooplankton in field samples. Limnol. Oceanogr. Methods **7:** 585–594.

Ferguson, R. I., and M. Church. 2004. A simple universal equation for grain settling velocity. J. Sediment Res. **74:** 933–937, doi:10.1306/051204740933

Frangoulis, C., E. D. Christou, and J. H. Hecq. 2005. Comparison of marine copepod outfluxes: Nature, rate, fate and role in the carbon and nitrogen cycles. Adv. Mar. Biol. **47:** 253–309, doi:10.1016/S0065-2881(04)47004-7

———, and others. In press. Connecting export fluxes to plankton food-web efficiency in the Black Sea waters inflowing into the Mediterranean Sea. J. Plankton Res. doi:10.1093/plankt/fbq010

Friedrichs, C. T. 2009. York River physical oceanography and sediment transport. J. Coast. Res. **57:** 17–22, doi:10.2112/1551-5036-57.sp1.17

———, L. D. Wright, D. A. Hepworth, and S. C. Kim. 2000. Bottom-boundary-layer processes associated with fine sediment accumulation in coastal seas and bays. Cont. Shelf Res. **20:** 807–841, doi:10.1016/S0278-4343(00)00003-0

Geptner, M. V., A. N. Zaikin, and Y. A. Rudyakov. 1990. Dead copepods in plankton: Facts and hypotheses. Oceanology **30:** 99–102.

Gomez-Gutierrez, J., W. T. Peterson, A. De Robertis, and R. D. Brodeur. 2003. Mass mortality of krill caused by parasitoid ciliates. Science **301:** 339, doi:10.1126/science.1085164

Greenlaw, C. F. 1977. Backscattering spectra of preserved zooplankton. J. Acoust. Soc. Am. **62:** 44–52, doi:10.1121/1.381503

Gries, T., and H. Güde. 1999. Estimates of the nonconsumptive mortality of mesozooplankton by measurement of sedimentation losses. Limnol. Oceanogr. **44:** 459–465, doi:10.4319/lo.1999.44.2.0459

Hall, L. W., M. C. Ziegenfuss, R. D. Anderson, and W. D. Killen. 1995. Use of estuarine water column tests for detecting toxic conditions in ambient areas of the Chesapeake Bay watershed. Environ. Toxicol. Chem. **14:** 267–278, doi:10.1002/etc.5620140212

Harris, R., P. Wiebe, J. Lenz, H. R. Skjoldal, and M. Huntley. 2000. ICES zooplankton methodology manual. Academic Press.

Heidelberg, J. F., K. B. Heidelberg, and R. R. Colwell. 2002. Bacteria of the γ-Subclass *Proteobacteria* associated with zooplankton in Chesapeake Bay. Appl. Environ. Microbiol. **68:** 5498–5507, doi:10.1128/AEM.68.11.5498-5507.2002

Heinle, D. R. 1966. Production of a calanoid copepod, *Acartia tonsa*, in the Patuxent River estuary. Chesapeake Sci. **7:** 59–74, doi:10.2307/1351126

Hirst, A. G., and T. Kiørboe. 2002. Mortality in marine planktonic copepods: Global rates and patterns. Mar. Ecol. Prog. Ser. **230:** 195–209, doi:10.3354/meps230195

Jenny, H., S. P. Gessel, and F. T. Bingham. 1949. Comparative study of decomposition rates of organic matter in temperate and tropical regions. Soil Sci. **68:** 419–432, doi:10.1097/00010694-194912000-00001

Jonsson, P. R., and P. Tiselius. 1990. Feeding behaviour, prey detection and capture efficiency of the copepod *Acartia tonsa* feeding on planktonic ciliates. Mar. Ecol. Prog. Ser. **60:** 35–44, doi:10.3354/meps060035

Kim, S. C., C. T. Friedrichs, J. P. Y. Maa, and L. D. Wright. 2000. Estimating bottom stress in tidal boundary layer from acoustic Doppler velocimeter data. J. Hydraul. Eng. **126:** 399–406, doi:10.1061/(ASCE)0733-9429(2000)126:6(399)

Kimmerer, W. J., and A. D. McKinnon. 1990. High mortality in a copepod population caused by a parasitic dinoflagellate. Mar. Biol. **107:** 449–452, doi:10.1007/BF01313428

Knutsen, T., W. Melle, and L. Calise. 2001. Determining the mass density of marine copepods and their eggs with a critical focus on some of the previously used methods. J. Plankton Res. **23:** 859–873, doi:10.1093/plankt/23.8.859

Køgeler, J. W., S. Falk-Petersen, Å. Kristensen, F. Pettersen, and J. Dalen. 1987. Density and sound speed contrasts in sub-arctic zooplankton. Polar Biol. **7:** 231–235, doi:10.1007/BF00287419

Lee, B. G., and N. S. Fisher. 1994. Effects of sinking and zooplankton grazing on the release of elements from planktonic debris. Mar. Ecol. Prog. Ser. **110:** 271–281, doi:10.3354/meps110271

Marshall, H. G. 2009. Phytoplankton of the York River. J. Coast. Res. **57:** 59–65, doi:10.2112/1551-5036-57.sp1.59

Mauchline, J. 1998. The biology of calanoid copepods. Adv. Mar. Biol. 33, doi:10.1016/S0065-2881(08)60234-5

McKee, M. H., F. J. Wrona, G. J. Scrimgeour, and J. M. Culp. 1997. Importance of consumptive and non-consumptive prey mortality in a coupled predator-prey system. Freshw. Biol. **38:** 193–201, doi:10.1046/j.1365-2427.1997.00205.x

Morgan, C. A., J. R. Cordell, and C. A. Simensted. 1997. Sink or swim? Copepod population maintenance in the Columbia River estuarine turbidity-maxima region. Mar. Biol. **129:** 309–317, doi:10.1007/s002270050171

Norland, S. 1993. The relationship between biomass and volume of bacteria, p.303–307. *In* P. F. Kemp, B. F. Sherr, E. B. Sherr and J. J. Cole [eds.], Handbook of methods in aquatic microbial ecology. Lewis Publishers.

Olson, R. K. 1963. Energy storage and the balance of producers and decomposers in ecological systems. Ecology **44:** 322–331, doi:10.2307/1932179

Orton, P. M., and G. C. Kineke. 2001. Comparing calculated and observed vertical suspended-sediment distributions from a Hudson River estuary turbidity maximum. Estuar. Coast. Shelf Sci. **52:** 401–410, doi:10.1006/ecss.2000.0747

Petersen, J. E., L. P. Sanford, and W. M. Kemp. 1998. Coastal plankton responses to turbulent mixing in experimental ecosystems. Mar. Ecol. Prog. Ser. **171:** 23–41, doi:10.3354/meps171023

Pond, D., and G. L. Pickard. 1983. Introductory dynamical oceanography. Pergamon.

Purcell, J. E., F. P. Cresswell, D. G. Cargo, and V. S. Kennedy. 1991. Differential ingestion and digestion of bivalve larvae by the scyphozoan *Chrysaora quinquecirrha* and by the ctenophore *Mnemiopsis leidyi*. Biol. Bull. **180:** 103–111, doi:10.2307/1542433

———, T. A. Shiganova, M. B. Decker, and E. D. Houde. 2001. The ctenophore *Mnemiopsis* in native and exotic habitats: U.S. estuaries versus the Black Sea basin. Hydrobiologia **451:** 145–176, doi:10.1023/A:1011826618539

———, J. R. White, and M. R. Roman. 1994. Predation by gelatinous zooplankton and resource limitation as potential controls of *Acartia tonsa* copepod populations in Chesapeake Bay. Limnol. Oceanogr. **39:** 263–278, doi:10.4319/lo.1994.39.2.0263

Reay, W. G., and K. A. Moore. 2009. Introduction to the Chesapeake Bay National Estuarine Research Reserve in Virginia. J. Coast. Res. **57:** 1–9, doi:10.2112/1551-5036-57.sp1.1

Roden, E. E., J. H. Tuttle, W. R. Boynton, and W. M. Kemp. 1995. Carbon cycling in mesohaline Chesapeake Bay sediments, 1: POC deposition rates and mineralization pathways. J. Mar. Res. **53:** 799–819, doi:10.1357/0022240953213025

Roman, M. R., D. V. Holliday, and L. P. Sanford. 2001. Temporal and spatial patterns of zooplankton in the Chesapeake Bay turbidity maximum. Mar. Ecol. Prog. Ser. **213:** 215–227, doi:10.3354/meps213215

Sampei, M., H. Sasaki, H. Hattori, A. Forest, and L. Fortier. 2009. Significant contribution of passively sinking copepods to the downward export flux in Arctic waters. Limnol. Oceanogr. **54:** 1894–1900.

Schultz, G. E. 1999. Bacterial dynamics and community structure in the York River estuary. Ph.D. thesis. College of William and Mary.

Scully, M. E., and C. T. Friedrichs. 2003. The influence of asymmetries in overlying stratification on near-bed turbulence and sediment suspension in a partially mixed estuary. Ocean Dyn. **53:** 208–219, doi:10.1007/s10236-003-0034-y

Seiwell, H. R., and G. E. Seiwell. 1938. The sinking of decomposing plankton in sea water and its relationship to oxygen consumption and phosphorus liberation. Proc. Am. Philos. Soc. **78:** 465–481.

Steinberg, D. K., and R. H. Condon. 2009. Zooplankton of the York River. J. Coast. Res. **57:** 66–79, doi:10.2112/1551-5036-57.sp1.66

Tang, K. W. 2005. Copepods as microbial hotspots in the ocean: Effects of host feeding activities on attached bacteria. Aquat. Microb. Ecol. **38:** 31–40, doi:10.3354/ame038031

———, S. L. Bickel, C. Dziallas, and H. P. Grossart. 2009. Microbial activities accompanying decomposition of cladoceran and copepod carcasses under different environmental conditions. Aquat. Microb. Ecol. **57:** 89–100, doi:10.3354/ame01331

———, C. S. Freund, and C. L. Schweitzer. 2006*a*. Occurrence of copepod carcasses in the lower Chesapeake Bay and their decomposition by ambient microbes. Estuar. Coast. Shelf Sci. **68:** 499–508, doi:10.1016/j.ecss.2006.02.021

———, K. M. L. Hutalle, and H. P. Grossart. 2006*b*. Microbial abundance, composition and enzymatic activity during decomposition of copepod carcasses. Aquat. Microb. Ecol. **45:** 219–227, doi:10.3354/ame045219

Terazaki, M., and M. Wada. 1988. Occurrence of large numbers of carcasses of the large, grazing copepod *Calanus cristatus* from the Japan Sea. Mar. Biol. **97:** 177–183, doi:10.1007/BF00391300

van der Meeren, T., R. E. Olsen, K. Hamre, and H. J. Fyhn. 2008. Biochemical composition of copepods for evaluation of feed quality in production of juvenile marine fish. Aquaculture **274:** 375–397, doi:10.1016/j.aquaculture.2007.11.041

van Rijn, L. C. 1993. Principles of sediment transport in rivers, estuaries and coastal seas. Aqua Publications.

Waggett, R., and J. H. Costello. 1999. Capture mechanisms used by the lobate ctenophore, *Mnemiopsis leidyi*, preying on the copepod *Acartia tonsa*. J. Plankton Res. **21:** 2037–2052, doi:10.1093/plankt/21.11.2037

Wider, R. K., and G. E. Lang. 1982. A critique of the analytical methods used in examining decomposition data obtained from litter bags. Ecology **63:** 1636–1642, doi:10.2307/1940104

Zajączkowski, M., and J. Legeżyńska. 2001. Estimation of zooplankton mortality caused by an Arctic glacier outflow. Oceanologia **43:** 341–351.

Associate editor: Mikhail V. Zubkov

Received: 22 December 2009
Accepted: 04 May 2010
Amended: 21 May 2010